J|A|C|S
ARTICLES
Published on Web 02/14/2006

Self-Assembly of PbTe Quantum Dots into Nanocrystal Superlattices and Glassy Films

Jeffrey J. Urban,*,†,‡ Dmitri V. Talapin,† Elena V. Shevchenko,†,§ and Christopher B. Murray*,†

Contribution from the IBM T.J. Watson Research Center, Nanoscale Materials and Devices Group, 1101 Kitchawan Road, Yorktown Heights, New York 10598, Department of Chemistry, Michigan State University, East Lansing, Michigan 48823, and Department of Applied Physics & Applied Mathematics, Columbia University, 200 SW Mudd Building, 500 West 120th Street, New York, New York 10027

Received December 6, 2005; E-mail: urban@post.harvard.edu; cbmurray@us.ibm.com

Abstract: Monodisperse lead telluride (PbTe) nanocrystals ranging from ~4 to 10 nm in diameter are synthesized to provide quantum dot building blocks for the design of novel materials for electronic applications. Two complementary synthetic approaches are developed that enable either (1) isolation of small quantities of nanocrystals of many different sizes or (2) the production of up to 10 g of a single nanocrystal size. PbTe nanocrystals are characterized by transmission electron microscopy (TEM), X-ray diffraction (XRD), and optical absorption. Assembly of PbTe nanocrystals is directed to prepare nanocrystal solids that display either short-range (glassy solids) or long-range (superlattices) packing order by varying deposition conditions. Film order and average interparticle spacing are analyzed with grazing-incidence small-angle X-ray scattering (GISAXS) and high-resolution scanning electron microscopy (HRSEM). We perform the first optical and electronic studies of PbTe solids and demonstrate that chemical activation of these films enhances conductivity by ~9−10 orders of magnitude while preserving their quantum dot nature.

Introduction

Nanomaterials display unique size-tunable physical and chemical properties distinct from their parent bulk compounds.[1,2] Specifically, in semiconductor nanocrystals, the size-tunable electronic and optical properties have their origins in "quantum confinement", the fact that quantum dots may be synthesized whose radius (r) is comparable to or smaller than the Bohr exciton radius (a_B).[3] Harnessing this nanoscale tunability on a macroscopic length scale could provide exciting new classes of materials for scientific and technological applications. One method to produce these "quantum dot solids" involves the self-organization of individual quantum dot building blocks into two- (2D) and three-dimensional (3D) macroscopic assemblies.[4−6] These nanocrystal solids can have their properties further modified by chemical treatments that optimize the interparticle spacing, passivate electronic traps, or introduce electronic dopants.

Constructing semiconductor nanocrystal solids requires highly tunable nanocrystal building blocks whose properties may be rationally designed. Therefore, it is critical to synthesize and study materials existing in the limit of strong-quantum confinement ($r \ll a_B$), as exemplified by the IV−VI lead chalcogenide quantum dots. These materials, whose excitonic Bohr radii (a_B) range from 20 (PbS) to 46 nm (PbTe),[7] present a degree of confinement not possible in many traditional II−VI and III−V systems whose a_B's typically range from ~1 to 10 nm.[7] Synthetic,[8,9] optical,[7,10] and electronic[11,12] experiments on two members of this family, PbS[13] and PbSe,[11,12] have generated significant scientific and technological interest. IV−VI quantum dots could provide useful materials for solar cell,[13] light-harvesting,[14] and telecommunication applications[15] because their large quantum confinement and small band gaps provide materials with size-tunable properties in the near-IR. This family of materials also shares flat, multivalley bandstructures and phonon dispersion relationships that enable fundamental studies of the size dependence of vibrational modes and phonon

† IBM T.J. Watson Research Center.
‡ Michigan State University.
§ Columbia University.

(1) Murray, C. B.; Kagan, C. R.; Bawendi, M. G. *Annu. Rev. Mater. Sci.* **2000**, *30*, 545.
(2) Alivisatos, A. P. *J. Phys. Chem.* **1996**, *100*, 13226.
(3) Brus, L. E. *J. Chem. Phys.* **1984**, *80*, 4403.
(4) Redl, F. X.; Cho, K.-S.; Murray, C. B.; O'Brien, S. *Nature* **2003**, *423*, 968.
(5) Shevchenko, E. V.; Talapin, D. V.; O'Brien, S.; Murray, C. B. *J. Am. Chem. Soc.* **2005**, *127*, 8741.
(6) Springholz, G.; Holy, V.; Pinczolits, M.; Bauer, G. *Science* **1998**, *282*, 734.
(7) Wise, F. W. *Acc. Chem. Res.* **2000**, *33*, 773.
(8) Cho, K.-S.; Talapin, D. V.; Gaschler, W.; Murray, C. B. *J. Am. Chem. Soc.* **2005**, *127*, 7140.
(9) Murray, C. B.; Sun, S.; Gaschler, W.; Doyle, H.; Betley, T. A.; Kagan, C. R. *IBM J. Res. Dev.* **2001**, *45*, 47.
(10) Du, H.; Chen, C.; Krishnan, R.; Krauss, T. D.; Harbold, J. M.; Wise, F. W.; Thomas, M. G.; Silcox, J. *Nano Lett.* **2002**, *2*, 1321.
(11) Talapin, D. V.; Murray, C. B. *Science* **2005**, *310*, 86.
(12) Romero, H. E.; Drndic, M. *Phys. Rev. Lett.* **2005**, *95*, 156801.
(13) McDonald, S. A.; Konstantatos, G.; Zhang, S.; Cyr, P. W.; Klem, E. J. D.; Levina, L.; Sargent, E. H. *Nat. Mater.* **2005**, *4*, 138.
(14) Schaller, R. D. a. K.; V. I. *Phys. Rev. Lett.* **2004**, *92*, 186601.
(15) Harrison, M. T.; Kershaw, S. V.; Burt, M. G.; Rogach, A. L.; Kornowski, A.; Eychmuller, A.; Weller, H. *Pure Appl. Chem.* **2000**, *72*, 295.

 10.1021/ja058269b CCC: $33.50

confinement, exciton−phonon coupling, and optical nonlinearities.[7,16]

Lead telluride, with a larger average excitonic Bohr radius (∼46 nm) and lighter e^- and h^+ masses (0.22 and 0.24 m_0, respectively)[17] than PbSe, is potentially even more size tunable than PbSe and a more promising candidate from which to build electronically active solids because of its large dielectric constant ($\epsilon_0 \sim 1000$), which should substantially reduce the Coulomb charging energy of the PbTe nanocrystal array.[17] In addition to these general considerations, the large anisotropy inherent to the bandstructure of PbTe ($a_{B\|} \sim 12$, $a_{B\perp} \sim 150$ nm) renders PbTe quantum dots a uniquely interesting subject for optoelectronic investigations and shape engineering of quantum properties. PbTe is also particularly promising for the further development of future direct energy conversion, thermophotovoltaic, and high-ZT thermoelectric devices.[18,19] Indeed, bulk PbTe possesses a high thermoelectric figure of merit and is currently an established material in both thermoelectric cooling and high-temperature power generation modules.[20] Moreover, nanocrystalline PbTe is predicted to benefit from changes in the electronic density of states and phonon scattering inherent to nanostructures, which would dramatically enhance the performance of PbTe for thermoelectric and energy generation applications.[20,21]

This manuscript reports the solution-phase synthesis of monodisperse, defect-free PbTe nanocrystals and nanocrystal solids derived from them. The size tunability and solution processability of these nanocrystals present distinct advantages relative to earlier work on lead chalcogenide quantum dots in glasses.[22−24] Our approach provides versatility, as any system from individual particles to controlled ensembles may be prepared and investigated. Additionally, this procedure enables facile and reliable size tuning of the nanocrystals employing either ligand- or time-based strategies. Optimizing these two complementary strategies enables the synthesis of either approximately milligram quantities of nanocrystal populations whose size is continuously increasing (time-based approach) or multigram quantities (up to ∼10 g scale) of nanocrystals of one chosen size (ligand-based approach). The excellent uniformity of these PbTe nanocrystals allows the creation of self-assembled structures with different types of order over different length scales. By manipulating deposition conditions, either nanocrystal superlattices or glassy films may be formed. Patterning of nanocrystal solids over approximately millimeter length scales is exploited to characterize and engineer the electronic properties of PbTe films, transforming them from insulators to conductors via chemical activation.

(16) Krauss, T.; Wise, F. W. *Phys. Rev. Lett.* **1997**, *79*, 5102.
(17) *Landolt-Bornstein*; Springer-Verlag: Berlin, 1983; Vol. 17.
(18) Heremans, J. P.; Thrush, C. M.; Morelli, D. T. *Phys. Rev. B* **2004**, *70*, 115334.
(19) Harman, T. C.; Taylor, P. J.; Walsh, M. P.; LaForge, B. E. *Science* **2002**, *297*, 2229.
(20) Rowe, D. M. *CRC Handbook of Thermoelectrics*; CRC Press LLC: Boca Raton, FL, 1995.
(21) Nolas, G. S.; Sharp, J.; Goldsmid, H. J. *Thermoelectrics: basic principles and new materials developments*; Springer: New York, 2001; Vol. 45.
(22) Craievich, A. F.; Kellermann, G.; Barbosa, L. C.; Alves, O. L. *Phys. Rev. Lett.* **2002**, *89*, 235503.
(23) Borrelli, N. F.; Smith, D. W. *J. Non-Cryst. Solids* **1994**, *180*, 25.
(24) Lipovskii, A.; Kolobkova, E.; Petrikov, V.; Kang, I.; Olkhovets, A.; Krauss, T.; Thomas, M.; Silcox, J.; Wise, F.; Shen, Q.; Kycia, S. *Appl. Phys. Lett.* **1997**, *71*, 3406.

Experimental Section

Chemicals. All manipulations are carried out using standard Schlenk line techniques under dry nitrogen. Tri-*n*-octylphosphine (henceforth referred to as TOP, Aldrich, 90%), amorphous tellurium shot (Aldrich, 99.999%), squalane (Aldrich, 99%), lead acetate trihydrate (Aldrich), and oleic acid (Aldrich, 90%) are used as purchased without further purification. Anhydrous hexanes, ethanol, chloroform, and trichloroethylene are purchased from a variety of sources and used without further purification. Trioctylphosphine telluride (0.75 M, TOPTe) is prepared by dissolving 9.57 g of tellurium shot in 100 mL of TOP with moderate stirring. The TOPTe solution described above is prepared and stored in a nitrogen glovebox.

Ligand-Based Synthesis of PbTe Nanocrystals. A typical synthetic protocol in which the relative ratio of lead oleate to lead acetate is manipulated to control size is described below for the synthesis of ∼7 nm PbTe nanocrystals: 1.1379 g of lead acetate trihydrate (3 mmol) and 2 mL of oleic acid (9 mmol) is dissolved in 20 mL of squalane. This solution is then heated under vacuum at 70 °C for 3 h to promote both the formation of lead oleate and the removal of adventitious water and acetic acid formed. The reaction flask is flushed with nitrogen, and the temperature is raised to 180 °C. At 180 °C, 12 mL of 0.75 M TOPTe solution is injected into the reaction mixture, which is subsequently maintained at 155−160 °C for 2 min. The reaction is then cooled to room temperature using a water bath to allow for isolation and purification of nanocrystals. To synthesize nanocrystals of different sizes, only the oleic acid/lead acetate ratio is adjusted according to the chart shown in Figure 1d.

Time-Based Synthesis of PbTe Nanocrystals. The use of reaction time to control nanocrystal size is demonstrated here by synthesizing 4.5 nm PbTe nanocrystals using a ligand concentration optimized to produce 5 nm nanocrystals under ligand-based conditions. A typical synthetic protocol for the synthesis of ∼4.5 nm PbTe nanocrystals is as follows: 1.1379 g of lead acetate trihydrate (3 mmol) and 1.0 mL of oleic acid (4.5 mmol) are dissolved in 20 mL of squalane. This solution is then heated under vacuum at 70 °C for 3 h and then flushed with nitrogen as before. Next, the temperature is raised to 180 °C and 12 mL of 0.75 M TOPTe solution is injected into the reaction mixture. The reaction is then maintained at 155−160 °C for 1 min and then promptly cooled to room temperature using a water bath. Once at room temperature, nanocrystal isolation and purification may be performed. To synthesize 5 nm nanocrystals under these conditions, the same procedure is followed, but the reaction is allowed to remain at the growth temperature for an additional minute, which effectively reproduces the standard ligand-based growth conditions.

Isolation and Purification of Nanocrystals. To isolate and purify the nanocrystals, the crude solution is first mixed with an equal volume of hexane. Next, the nanocrystals are precipitated by adding ethanol and the centrifuging resultant mixture at 3836*g* for 4 min. A black pellet of PbTe nanocrystals is isolated by pouring off the supernatant solution. The resulting nanocrystals are then resuspended in chloroform, hexanes, toluene, tetrachloroethylene, or several other solvents to form stable colloidal solutions.

Assembly of Nanocrystal Films. The assembly of nanocrystal solids generally proceeds via controlled evaporation of a concentrated nanocrystal solution onto a substrate. Typical substrates are either Si/SiO_2 chips whose surface is modified with hexamethyl disilazane (HMDS) at 150 °C for 30 min prior to nanocrystal deposition, silicon nitride membranes, or amorphous carbon-coated transmission electron microscopy (TEM) grids. Solvent choice allows us to adjust the packing properties of the PbTe nanocrystals in the resultant solids. Densely packed nanocrystal superlattices are formed by drop casting PbTe nanocrystals from a solution of trichloroethylene, whereas dispersing nanoparticles from chloroform results in densely packed glassy films that possess only local order. In contrast to earlier reports, slowing the drying process by decreasing the solvent evaporation rate did not create

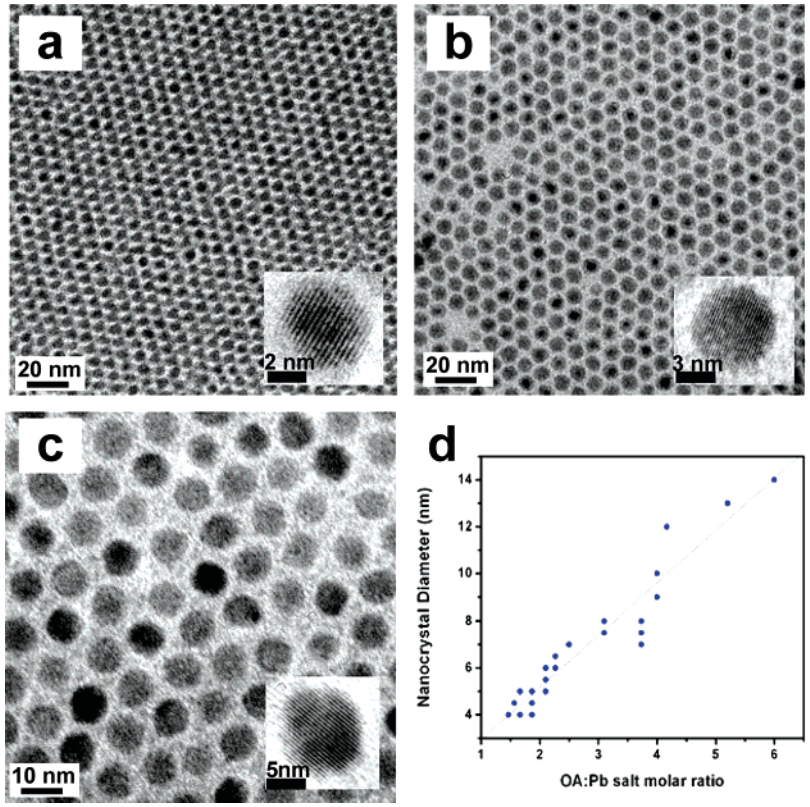

Figure 1. TEM images of PbTe nanocrystals of different sizes. (a), (b), and (c) show images of small (5.0 nm, $\sigma = 5.5\%$), medium (6.5 nm, $\sigma = 4.4\%$), and large (8.2 nm, $\sigma = 5.2$) nanocrystals, respectively. These low-magnification pictures demonstrate the uniformity in size and shape of the nanocrystals. The insets of (a)−(c) show representative high-resolution TEM (HRTEM) images of individual nanocrystals from each of these samples, demonstrating the high crystallinity and shape evolution of the nanocrystals. (d) Plot of nanocrystal diameter vs oleic acid to lead salt molar ratio from over 30 separate syntheses. There is a good correlation between nanocrystal size and oleic acid concentration.

long-range order but surprisingly generated only locally ordered (glassy) films. For example, uniform, glassy PbTe films were cast from a solution of PbTe nanocrystals in a hexane/octane (~8:1 volumetric ratio) mixture and a similar dispersion in pentane showed a high degree of local ordering. Information on interparticle spacing and, more globally, on the degree of ordering of the nanocrystalline films was obtained by grazing-incidence small-angle X-ray scattering (GISAXS). The film thickness can be tailored by adjusting the concentration and the volume of the nanocrystal solution cast per area unit.

Sample Characterization. Transmission electron microscopy (TEM), high-resolution TEM (HRTEM), powder X-ray diffraction (XRD), energy-dispersive X-ray spectroscopy (EDS), and near-IR absorption spectroscopy are used to characterize the size, shape, structure, composition, and optical properties of the PbTe nanocrystals. Characterization of particle ordering and interparticle spacing in the PbTe films is performed via small-angle X-ray scattering at grazing incidence using a D8 Discover Series II diffractometer (Bruker) with a 2D area detector. A copper anode was used as the radiation source (the acceleration voltage was 40 kV, and the flux was 40 mA), and the signal integration time varied from 10 to 60 min. The angle of incidence was typically 0.83°, slightly greater than the critical angle of the nanocrystal film.

The TEM and HRTEM images were obtained using a Philips CM-12 microscope operating at 120 kV. Samples for TEM analysis were prepared by depositing a drop of dilute nanocrystal solution in chloroform or pentane on a 400 mesh carbon-coated copper grid and allowing the solvent to evaporate at room temperature. Statistical analysis of the size distributions of the nanocrystals is obtained using Scion Image data processing software. TEM images of PbTe monolayers taken at various magnifications are converted into purely black and white images and processed using the particle analysis package in Scion Image. These data are then plotted and fit to a Gaussian, and the full-width at half-maximum of that Gaussian is used to calculate the standard deviation in particle diameter.

Near-IR absorption spectra were collected on trichloroethylene solutions of PbTe nanocrystals using a QualitySpec Pro IR spectrometer (Analytical Spectral Devices, Inc.). Wide-angle powder XRD measurements were performed on a Bruker D500 diffractometer operating in the Bragg−Brentano configuration with Co Kα radiation ($\lambda = 1.79$ Å) with scatter and diffraction slits of 1° and a 0.15 mm collection slit. Samples for wide-angle XRD measurements are prepared by depositing concentrated PbTe nanocrystal solutions in hexane onto a glass plate.

To study the electronic properties of PbTe nanocrystal assemblies, we deposited 40 ± 10 nm thick films of PbTe nanocrystals on 100 nm thick SiO_2 gate oxides thermally grown on heavily doped Si wafers used as the back gate.[11] Source and drain Ti/Au (75/375 Å) electrodes were patterned on the SiO_2 surface by lithography prior to depositing the nanocrystal film. Spacing between the source and drain electrodes was typically 10 μm; i.e., the typical path of charge carriers from the source to the drain electrode involved ~10^3 or more individual PbTe nanocrystals. Field-effect devices are tested using an Agilent 4156B semiconductor parameter analyzer. The source electrode was grounded. All room-temperature electrical measurements are performed under dry nitrogen atmosphere.

Results and Discussion

PbTe Nanocrystal Synthesis. As-prepared PbTe nanocrystals are monodisperse, as shown in Figure 1a−c, which displays TEM micrographs of three different sizes (5.0, 6.5, 8.2 nm) of monodisperse ($\sigma = 5.5\%$, 4.4%, 5.2%, respectively) PbTe nanocrystals isolated from raw reaction products without purification. Further size-selective processing techniques may

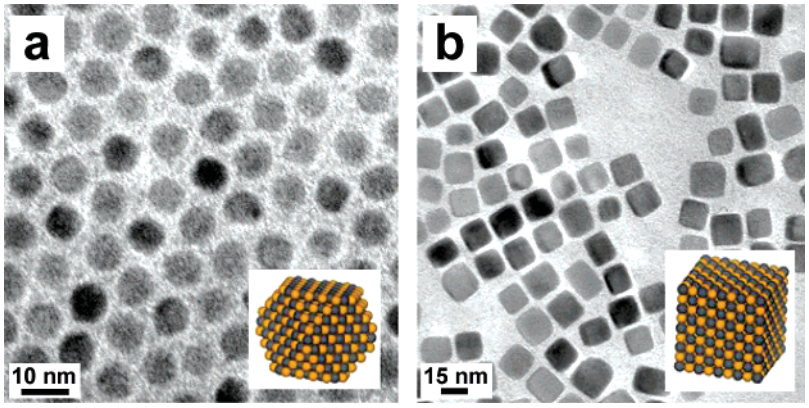

Figure 2. (a) TEM image of cuboctahedral 7.5 nm PbTe nanocrystals. The inset shows a model of a cuboctahedron composed of a rock-salt crystal. (b) TEM image of cubic PbTe nanocrystals >12 nm in size. The inset shows a model of a cube composed of a rock-salt crystal.

be employed to further narrow nanocrystal size distributions. We identify four parameters as the variables most useful for manipulating nanocrystal size and shape: reaction temperature, reaction time, reaction solvent, and ratio of ligand to metal salt. Reaction temperature directly impacts the rate of nanocrystal nucleation and growth and, indirectly, the shape of the nanocrystals. Generally, reactions conducted at <170 °C yield solutions of monodisperse cuboctahedral nanocrystals (Figure 2a) whereas reactions performed at >200 °C yield larger and more polydisperse cubic nanocrystals (Figure 2b). The observation that PbTe nanocrystals become more cubic in shape as they grow larger is true under all permutations of reaction conditions and can be understood in the context of a Wulff construction, as discussed in the next section.

The influence of the duration of time spent at the growth temperature is quite similar to that of the reaction temperature. For intermediate reaction times (~1.5−4 min), the size and shape of the nanocrystals are relatively insensitive to the precise length of time spent at the growth temperature. However, if a reaction is maintained at the growth temperature for extended (6−20 min) periods, the nanocrystals become polydisperse and the average feature size increases dramatically (~20 min reactions yield ~200−500 nm cubes). Conversely, stopping a reaction quickly after injection (30−50 s) produces nanocrystals whose average diameter (compared to the same reaction carried out for 2 min) is 10−20% smaller. However, the shorter reaction duration means that some precursors remain unreacted, and reaction yield is correspondingly reduced. On the basis of these observations, we conclude that the majority of nanocrystal growth occurs relatively quickly (<30 s) after injection. This introduces the possibility of optimizing growth conditions to isolate a sample of desired size after a fixed time period, with longer reaction times generally leading to larger nanocrystal sizes.

When dibenzyl ether is used as the solvent instead of squalane, the nanocrystals produced are consistently more cubic in shape. This trend is particularly pronounced at higher temperatures and longer reaction times, when sharp, faceted cubes of PbTe are produced. Despite providing easy access to a different morphology, dibenzyl ether was not pursued as reactions conducted in this solvent yield materials with a large standard deviation in size.

Ligand Concentration and PbTe Nanocrystal Size. Ligand-based reaction conditions allow nanocrystal size to be adjusted by changing the ratio of oleic acid to lead acetate, as shown in Figure 1d. This graph delineates the trend that larger nanocrystals are produced as the molar ratio of ligand/metal salt is increased. We hypothesize that this trend is due to the different reaction kinetics of lead acetate and lead oleate, which translate into changes in nucleation rates and particle size.[25,26] As the amount of oleic acid is increased, more lead oleate (relative to lead acetate) is formed in solution prior to TOPTe injection. As lead oleate is more stable than lead acetate, it reacts more slowly and produces a smaller number of larger nuclei that grow into large nanocrystals by consuming Pb and Te precursors. Conversely, for low oleic acid concentrations, a more quickly reacting lead acetate precursor leads to larger quantities of smaller nuclei and, ultimately, to smaller nanocrystals because there exists less Pb and Te feedstock per nucleus created. Although this hypothesis is corroborated by our experimental findings, further investigation is necessary and alternative mechanisms cannot be excluded at present.

We also identify a trend in crystal shape as a function of size. Figure 2b shows that crystals whose average feature size reaches ~10 nm become distinctly more cubic in shape. This shape evolution may be understood in the context of a Wulff construction, where the equilibrium crystal shape is determined by minimization of the surface free energy for a given volume.[27] In three-dimensional crystals whose underlying unit cell possesses cubic symmetry, this is known to correspond to a cubic shape.[27] This observation has also been made in previous studies of PbTe;[28,29] however, it is important to note that the Wulff construction argument presented here does not account for either ligand capping of crystalline facets and the concomitant energy modifications accompanying this process or kinetic arguments for this shape evolution.[28,29]

Size and Structural Analysis. Nanocrystal sizes are obtained using several complementary techniques that access different length scales. HRTEM micrographs (insets of Figure 1a−c) are obtained for 20−30 nanocrystals from each reaction, and the number of lattice planes is counted to determine the diameter of each nanocrystal. Lower-magnification TEM images (Figure 1a−c), which show the uniformity in particle size within each sample, are used for size-distribution analysis. Average particle

(25) Yin, Y.; Alivisatos, A. P. *Nature* **2005**, *437*, 664.
(26) Shevchenko, E. V.; Talapin, D. V.; Schnablegger, H.; Kornowski, A.; Haase, M.; Weller, H. *J. Am. Chem. Soc.* **2003**, *125*, 9090.
(27) Khare, S. V.; Kodambaka, S.; Johnson, D. D.; Petrov, I.; Greene, J. E. *Surf. Sci.* **2003**, *522*, 75.
(28) Lu, W.; Fang, J.; Stokes, K. L.; Lin, J. *J. Am. Chem. Soc.* **2004**, *126*, 11798.
(29) Lu, W.; Fang, J.; Ding, Y.; Wang, Z. L. *J. Phys. Chem. B* **2005**, *109*, 19219.

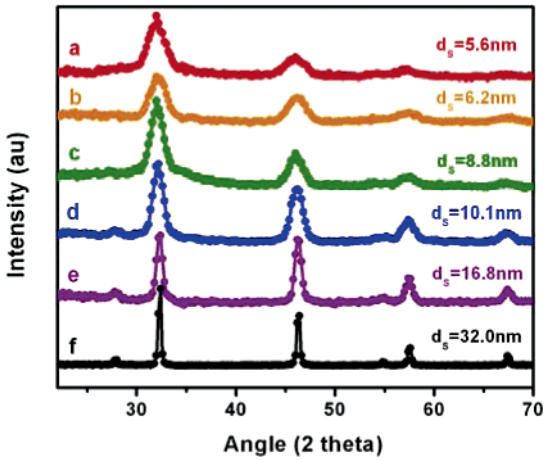

Figure 3. (a)−(f) XRD patterns obtained from powders composed of PbTe nanocrystals of different sizes. The sizes indicated in (a)−(f) are calculated values from the Scherrer equation based on analysis of the width of the [100] peak.

size information is also obtained by analyzing the line widths of X-ray diffraction patterns obtained from reaction products. The Scherrer formula relates the breadth (in 2Θ) of the diffraction peaks to the minimum feature size of a crystal (L): $\Delta 2\Theta = \lambda/L \cos \Theta$, where λ is the X-ray wavelength.[30] The average particle size obtained for the XRD patterns (Figure 3) closely corresponds to the information obtained from TEM images for nanocrystals smaller than ∼10 nm. However, the close correspondence between observed particle size in TEM and calculated particle size breaks down for larger nanocrystals. We attribute this difference between calculated and observed particle size to the increased polydispersity of cubic samples >10 nm in size discussed previously. More global information about particle size (length scale of ∼500 μm) is obtained through GISAXS measurements obtained on thin films of nanocrystals deposited on a silicon substrate. These measurements are discussed in a later section, although we note here that the interparticle spacings obtained from those measurements closely correspond to the TEM and XRD data.

Optical Properties of PbTe Nanocrystals. Reports of well-resolved optical absorption spectra from PbTe nanocrystals have been limited because of difficulties associated with preparing monodisperse PbTe nanocrystal samples and intrinsic physical properties unique to PbTe that broaden the excitonic transitions (Figure 4b).[31,32] Bulk PbTe has a direct band gap of 0.23 eV at room temperature at 4 equiv L points in the Brillouin zone.[17] Figure 4a shows well-resolved absorption spectra recorded on six different sizes of PbTe nanocrystals dispersed in trichloroethylene. The influence of strong quantum confinement is evident from Figure 4a, in which large absorption tunability >550 nm (∼180 meV) is exhibited over a small variation in nanocrystal diameter (∼5 nm). Figure 4b highlights the spectral broadening inherent to PbTe nanocrystals by comparing absorption spectra for comparably monodisperse samples of PbSe and PbTe nanocrystals of similar size. PbSe displays sharp, spectrally resolved excitonic transitions (fwhm ∼ 80 nm), whereas only broad transitions are discernible in PbTe (fwhm ∼ 150 nm).

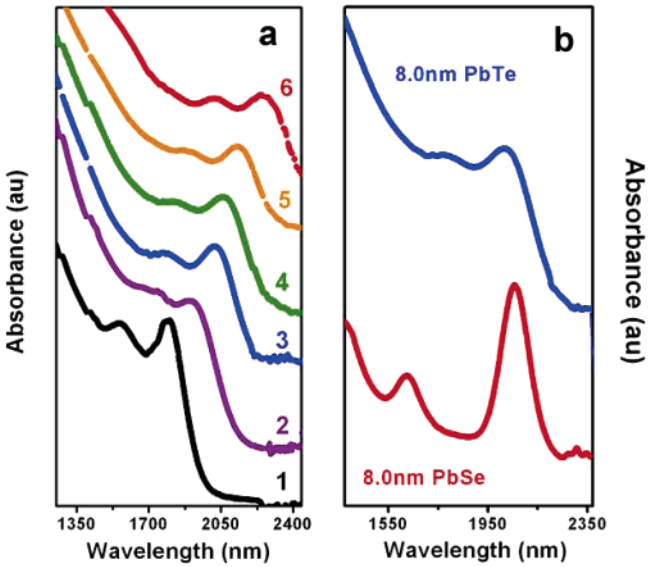

Figure 4. (a) Optical absorption spectra collected on PbTe nanocrystals of different sizes. Measured nanocrystal diameters corresponding to spectra 1−6 are 4.2, 5.5, 6.6, 7.5, 8.2, and 8.8 nm, respectively. (b) Demonstrates the spectral broadening inherent to PbTe nanocrystals by comparing absorption spectra measured from PbTe and PbSe samples of nearly identical size, shape, and size distribution.

As the sizes, shapes, size distributions, and band gaps of these PbSe and PbTe samples are nearly identical, another physical mechanism must contribute to this severe spectral broadening. This issue has been explored theoretically by both **k·p** and effective mass models;[7,31,32] however, it has proven difficult to treat with great precision theoretically and is still not entirely understood. Currently, the broad transitions in PbTe are thought to originate in both band mixing and the extreme anisotropy of the PbTe bandstructure near its 4-fold degenerate L point, which spread out the oscillator strengths over a greater energy range.[7,31] The synthesis of PbTe nanocrystals could enable studies directed toward resolving current debates surrounding the detailed understanding of the origin of optical transitions in lead chalcogenide systems.[33]

Assembly of Densely Packed PbTe Solids. The ability to form well-ordered, densely packed nanocrystal solids is an important step toward generating advanced materials for technological applications and physical measurements. Spatially patterning nanocrystals over long length scales (>100 particle diameters) is efficiently achieved by exploiting self-organization processes, as in well-known examples from thin films and superlattice solids.[4,5,34] Here, drop-casting methods are used to achieve different types of packing in PbTe nanocrystal solids. Nanoparticle ordering depends on the wetting properties, solvent evaporation rate, and morphology of the substrate. In principle, different types of packing in nanocrystal films can be achieved by changing the wetting properties and evaporation rate of the solvent, as demonstrated in Figures 5 and 6. Deposition of PbTe nanocrystals from a trichloroethylene solution onto a carbon-coated TEM grid results in superlattice formation (Figure 5a−c). However, these well-ordered hcp and fcc superlattices are not observed when particles are deposited from chloroform or hexane solutions. Ordering in these superlattices is excellent

(30) Guinier, A. *X-ray Diffraction In Crystals, Imperfect Crystals, and Amorphous Bodies*; Dover Publications: San Francisco, 1994.
(31) Turdury, G. E.; Marquezini, M. V.; Ferreira, L. G.; Barbosa, L. C.; Cesar, C. L. *Phys. Rev. B* **2000**, *62*, 7357.
(32) Kang, I.; Wise, F. W. *J. Opt. Soc. Am. B* **1997**, *14*, 1632.
(33) Liljeroth, P.; Zeijlmans van Emmichoven, P. A.; Hickey, S. G.; Weller, H.; Grandidier, B.; Allan, G.; Vanmaekelbergh, D. *Phys. Rev. Lett.* **2005**, *95*, 086801.
(34) Murray, C. B.; Kagan, C. R.; Bawendi, M. G. *Science* **1995**, *270*, 1335.

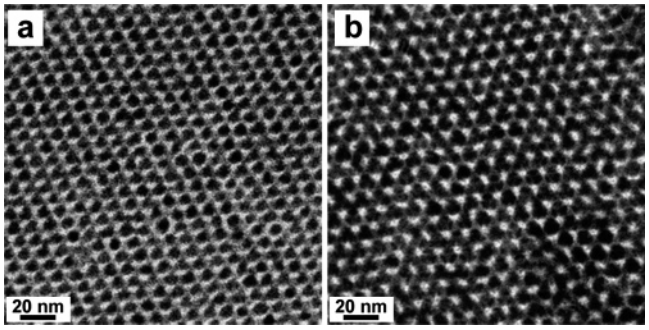

Figure 5. (a) and (b) show TEM images of superlattices formed from 5 and 7.5 nm PbTe nanocrystals, respectively.

over lengths of ~1 μm, which is good for some measurements, but of limited utility for electronic transport measurements requiring uniform ordering up to 50 μm length scales.

To create optimal PbTe nanocrystal solids for electronic measurements, packing uniformity over dimensions of ~2−50 μm is desired.[11] For these applications, glassy PbTe nanocrystal solids lacking grain boundaries and other discontinuities are formed by drop casting a solution of PbTe nanocrystals from a hexane/octane (~8:1 vol) mixture onto a Si/SiO_2 chip pretreated with HMDS. This chemical treatment transforms SiO_2 into a uniformly hydrophobic surface, which promotes the wetting and adhesion of deposited nanocrystals from solution. This procedure creates films of excellent uniformity in thickness and packing over approximately centimeter length scales, as indicated by the HRSEM image shown in Figure 6a. The inset of Figure 6a is a higher-magnification HRSEM image of the same film, demonstrating that these PbTe solids exhibit local order but lack long-range order. Forming densely packed, glassy solids is desirable for measurements where sample uniformity over large length scales is required, whereas polycrystalline superlattice solids of PbTe have unquantifiable contributions from grain boundaries, defects, and disorder. Analysis of the GISAXS patterns (Figure 6c) supports the conclusions made from the structural and microscopic analyses mentioned above. The presence of rings of uniform scattering intensity over all spatial dimensions in the GISAXS data is characteristic of glassy systems that possess good short-range order and frustrated long-range order. This is further confirmed by the broad peaks shown in the small-angle scattering data in Figure 8c.

PbTe solids deposited from pentane under oxygen- and moisture-free conditions, however, exhibit highly nonuniform crystalline order as shown in Figure 6b. This SEM shows PbTe superlattice islands of up to ~1 μm in diameter separated by channels of disorganized nanocrystal deposition. Comparison of the insets of 6a and 6b demonstrates the excellent ordering of the superlattice islands in the pentane-deposited solids, and the low-magnification SEM images reinforce how different the thickness and packing are between these samples over long length scales. Although these results are highly reproducible, they appear counterintuitive as slower evaporating solvents (e.g., hexane/octane) might be expected to encourage individual particles to find equilibrium positions and form solids with more long-range order whereas faster evaporating solvents (e.g., pentane) can constrain particles to deposit in less energetically favorable, nonequilibrium positions. Ultimately, we chose to use a hexane/octane mixture for our measurements because exerting control over interparticle spacing and film order is a critical element for the design of thin-film devices.

Electronic Characterization and Chemical Activation of PbTe Films. Current interest in low-cost alternatives to silicon technology for consumer electronics, radio frequency identification (RFID) tags, and sensors has spawned intense research on conducting organic polymers, which combine good device performance with easy processability. In principle, nanocrystal solids could provide superior materials for these applications by combining the intrinsically higher carrier mobilities from inorganic crystals with the facile solution processability of quantum dots. Such quantum dot solids could provide uniquely excellent electronic and optoelectronic materials, as they could combine both the tunable electronic properties of quantum dots with the collective charge transport characteristics of extended arrays of inorganic semiconductor solids.[35]

The pursuit of highly conductive, gateable semiconductor nanocrystal devices has been a very active, yet challenging, area of research.[11,12,36] Typically, these difficulties arise from a variety of factors: the presence of capping ligands which maintain large interparticle distances, dangling bonds that create mid-gap trap states, and low dielectric constants that result in large charging energies. Therefore, to generate conductive nanocrystal solids, it would be desirable to decrease interparticle spacing, prevent or fill trap states, and use semiconductors of high dielectric constant.[11] The strategy employed here entails the assembly of PbTe nanocrystals, which have an extremely high dielectric constant ($\epsilon_0 \sim 1000$), into quantum dot solids that are chemically activated by treatment with hydrazine, a chemical which was found to decrease interparticle spacing, passivate trap states, and dope the solid.[11]

Thin-film nanocrystal devices for electronic studies are created by depositing PbTe nanocrystals from a ~8:1 hexane/octane solution onto highly doped Si wafers with 100 nm thick SiO_2 thermal gate oxide. Source and drain Ti/Au (75/375 Å) electrodes (whose spacing was varied from 4 to 40 μm) were patterned on the SiO_2 surface prior to nanocrystal deposition, as depicted in Figure 7a. These films are characterized by GISAXS and SEM as discussed in the previous section. Electronic measurements show that as-deposited films are insulating, demonstrate no gate effect, and possess very low conductivities ($G \sim 10^{-13}$ S/cm^{-1}) as shown in Figure 7a. We attribute this poor conductivity primarily to the difficulty of charge transport associated with the large interparticle separations due to organic ligands. This view is supported by GISAXS measurements which report an average interparticle spacing of 1.8 nm (Figure 8c) for PbTe films composed of 7 nm nanocrystals (as measured by TEM). Further support comes from optical absorbance studies of nanocrystal films shown in Figure 8a, which indicate that the absorbance characteristics of nanocrystals in films are nearly identical to capped nanocrystals in solution.

PbTe films are then treated with a 1.0 M solution of hydrazine in acetonitrile overnight, washed with acetonitrile, dried, and measured again. After treatment, the same PbTe films show a ~10−12 order of magnitude increase in conductance and carry milliampere currents through ~10 μm long and 3000 μm wide channels. Also, these films now demonstrate gate-modulated

(35) Vanmaekelbergh, D.; Liljeroth, P. *Chem. Soc. Rev.* **2005**, *34*, 299.
(36) Ridley, B. A.; Nivi, B.; Jacobson, J. M. *Science* **1999**, *286*, 746.

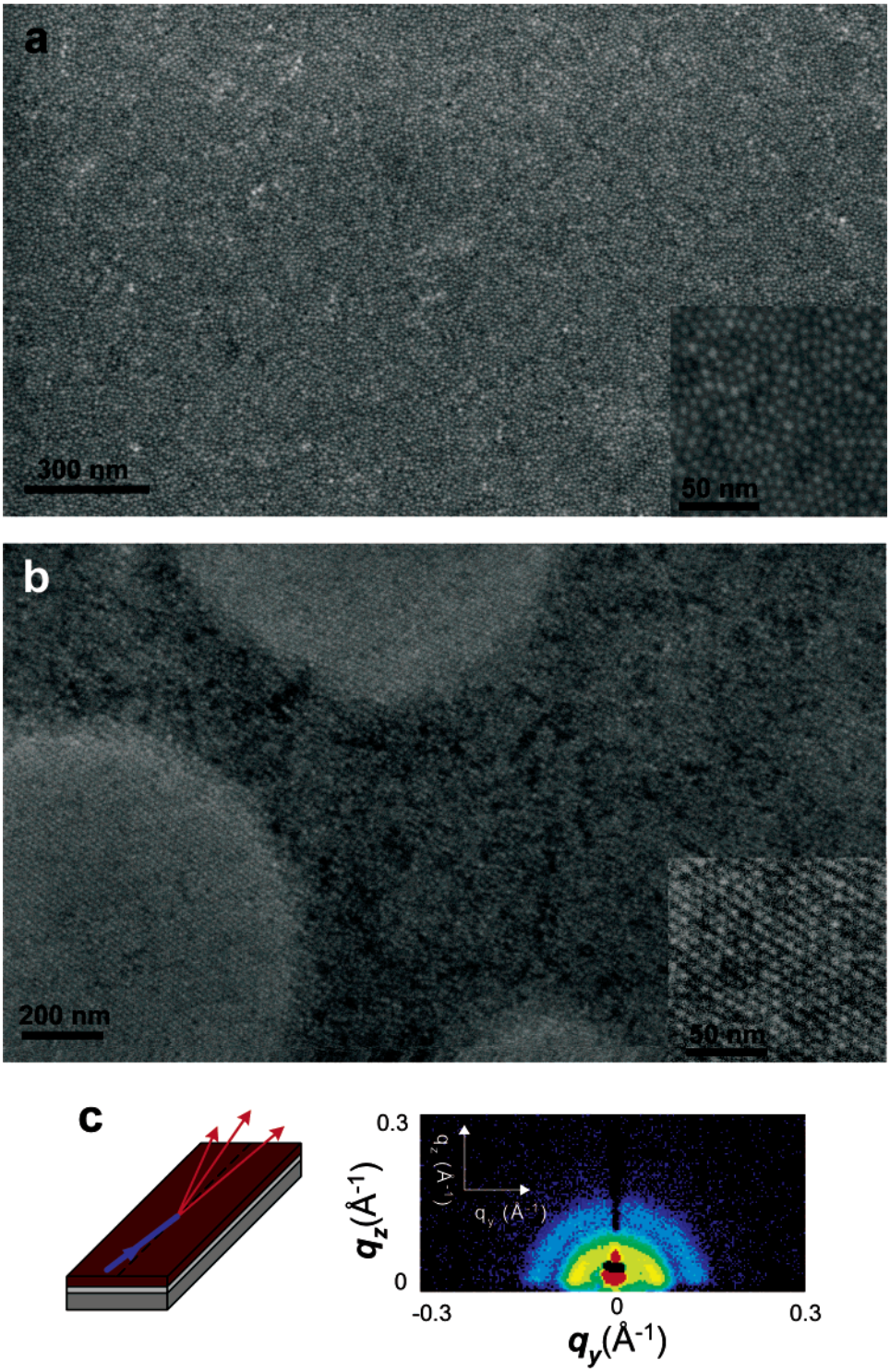

Figure 6. (a) SEM image of a glassy PbTe nanocrystal film deposited from hexane/ octane. This micrograph demonstrates the uniformity in film thickness and packing over long length scales. (b) SEM image of PbTe nanocrystal superlattice islands formed from pentane deposition. The insets to (a) and (b) show the extent of local ordering present in each of these films. (c) Cartoon of experimental geometry used in GISAXS experiments. (d) GISAXS pattern obtained from a PbTe nanocrystal film deposited from hexane/octane solvent mixture. q_y and q_z are lateral and vertical components of the momentum transfer, respectively.

currents characteristic of *n*-type channel FETs (Figure 7b). Hydrazine chemically activates the films by decreasing interparticle spacing through removal of the oleic acid groups and dopes these nanocrystal solids (evidenced by the *n*-type behavior in Figure 7c).[11] This proposal is corroborated by GISAXS measurements of the treated film, which show a decrease in interparticle spacing from 1.8 to 0.3 nm (Figure 8c). Furthermore, these films may be heated at moderate temperatures to further enhance their conductivity (Figure 7c), although caution is essential as excessive heat treatment destroys the original quantum dot identity of these solids (Figure 8b). Because the loss of quantum dot identity occurs at the same temperature at which film conductivity is greatly enhanced, we attribute these results to the change in packing density and density of states

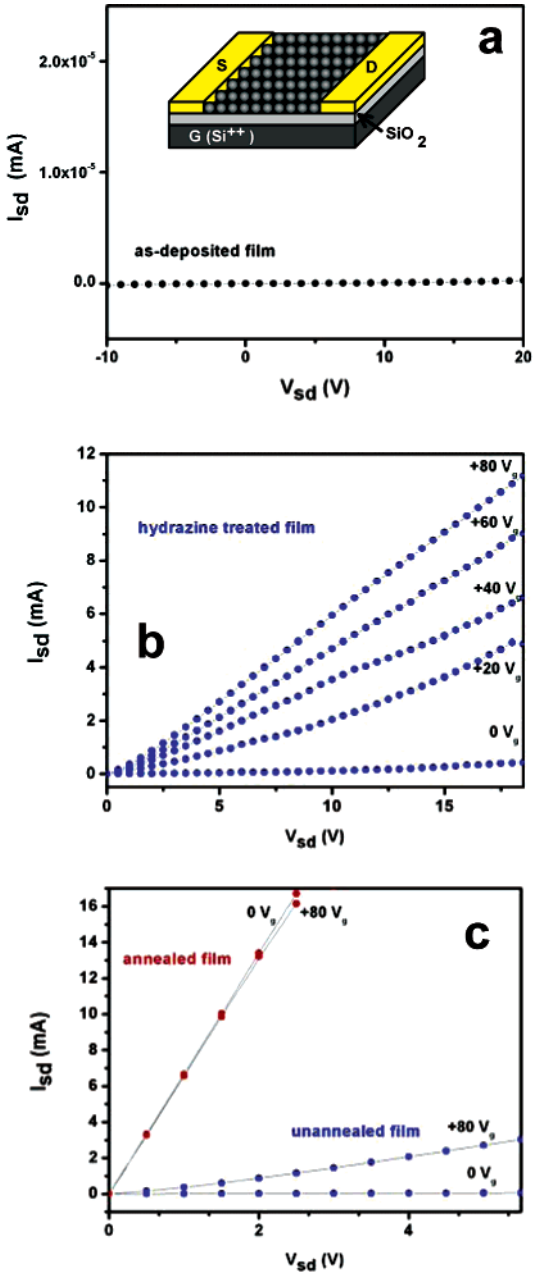

Figure 7. (a) I−V measurements of as-deposited PbTe nanocrystal films. These films are initially insulating and carry only approximately picoampere currents. The inset shows a cartoon of the measurement geometry. (b) I−V measurement of hydrazine-treated PbTe nanocrystal films. After chemical activation, these films behave as highly conductive *n*-type nanocrystal FETs. (c) Comparison of I−V characteristics of the nanocrystal film before and after annealing at 200 °C. Extended annealing of PbTe nanocrystal films enhances conductivity dramatically and produces behavior similar to that of a metal or degeneratively doped semiconductor.

between nanocrystal films and sintered, polycrystalline solid films. These preliminary results demonstrate the potential of

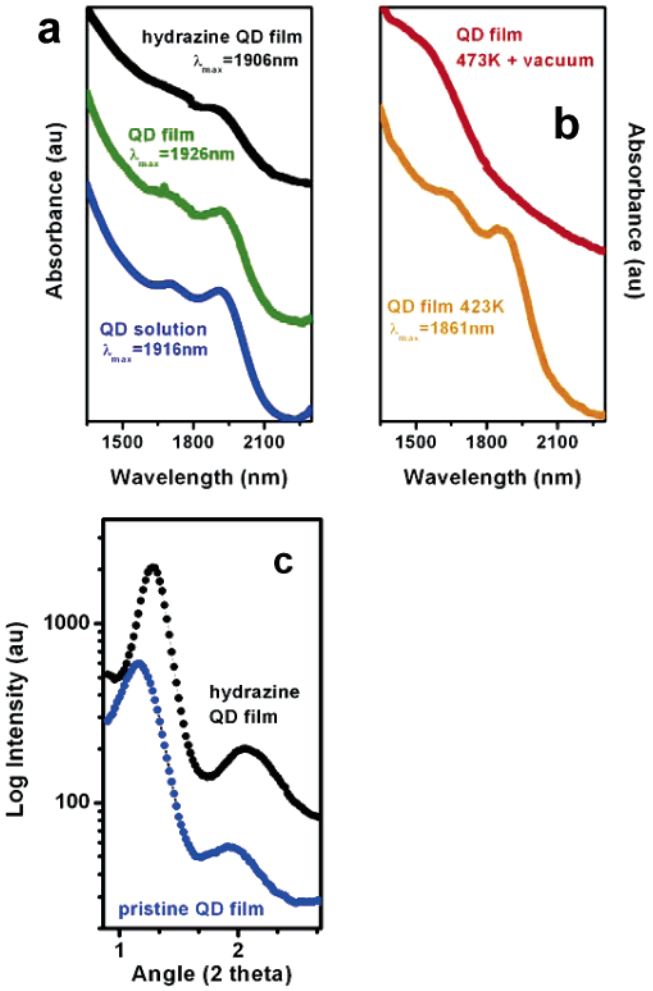

Figure 8. (a) Comparison of optical absorbance spectra recorded on nanocrystal solutions, as-deposited nanocrystal films, and hydrazine-treated films. Aside from a small red shift, there is no appreciable change in the spectra of as-deposited films, indicating that the nanocrystal nature of the individual dots is preserved in the film. (b) Absorbance spectra recorded from 423 K annealed and 473 K vacuum-annealed PbTe films. This figure shows the particulate nature of the film is maintained until vacuum annealing at 473 K. (c) Small-angle X-ray scattering from a film of 7 nm PbTe nanocrystals before (blue curve) and after (black curve) the hydrazine treatment. Hydrazine treatment decreases interparticle spacing by ∼1.8 nm, the approximate length of an oleic acid molecule.

thin-film nanocrystal solids for technological applications. Further studies are currently underway to completely characterize the electronic properties of these films and elucidate the role of hydrazine in chemical activation.

Acknowledgment. We thank Frank Wise, Sarah Cowan, and Ricardo Ruiz for helpful comments and discussions. This research was supported by ONR.

JA058269B